Quantum Physics Letters
An International Journal

http://dx.doi.org/10.18576/qpl/130101

Enhancing Local Field and Optical Bistability of Cylindrical Nanoinclusions Within Passive and Active Host Matrices

Shewa Getachew[1,*] *and Hawi Aboma*[2]

[1] Department of Physics, Wolkite University, Wolkite, Ethiopia
[2] Department of Electrical and Computer Engineering, Wolkite University, Wolkite, Ethiopia

Received: 12 Jan. 2024, Revised: 31 Jan. 2024, Accepted: 25 Feb. 2024
Published online: 1 Apr. 2024

Abstract: This study investigated the influence of the metal fraction and the real and imaginary components of the dielectric function of the host matrix on the local field enhancement and optical bistability (*OB*) of cylindrical nanoinclusions within both passive and active host matrices. By solving the Laplace equation in the quasi-static limit, we derived expressions for the electric potentials of the cylindrical nanoinclusions. These expressions were then integrated with the Lorentz-Drude model to obtain the equation for the enhancement factor within the core of the cylindrical nanoinclusions. The results demonstrate that composites comprising metal-coated dielectric nanoparticles experience a significant increase in the local field at two resonant frequencies as the metal fraction rises and the value of the imaginary part of the dielectric properties of the host matrix rises in active host matrices. Conversely, for nanoinclusions with dielectric-coated metal core, the enhancing local field factor notably increases only at one resonant frequency as the metal fraction decreases, while increasing the value of imaginary part in active host matrices. Additionally, the investigation shows that an increase in the metal fraction leads to an expansion of the bistable region of *OB*. Specifically, within passive and active host matrices, augmenting the metal fraction of metal covered dielectric nanoinclusions results in higher incident field requirements at each switching-up threshold point, leading to a broader bistable region. Moreover, we observed that the bistable area of *OB* in active host matrices of cylindrical core-shell nanoinclusions increases as the magnitude of the imaginary part of the dielectric function of the host matrix increases. The enhancement of electromagnetic wave properties opens up the potential for the emergence of nonlinear optical phenomena, such as optical bistability. Optical bistability plays a crucial role in applications related to optical communication and computing, such as optical sensing, optical switches, and memory elements.

Keywords: Nanoparticles, resonate frequency, nanoinclusions, host matrix, amplification

1 Introduction

Indeed, experts around the world are becoming increasingly interested in nanoparticles. Numerous studies have been initiated due to their distinct optical characteristics, which diverge markedly from those of larger bulk materials [1]. Metal-coated nanoparticles are particularly intriguing, as their optical properties are largely determined by the behavior of their surface electrons. The fluctuations of these surface electrons within the electric potential created by the electrically charged ionic core significantly affect the optical properties of the metal-coated dielectric nanoparticles [2, 3]. There are two main ways in which metals and dielectrics interact to regulate light in these systems. First, they reduce reflections through interference cancellation, allowing light to penetrate deeper into the metals. This also enables light localization, which enhances the nonlinear response [4,5]. The resonances of surface plasmons, which are collective electron oscillations along the surfaces of nanoparticles, are highly sensitive to the particle structures. The optical properties of nanoparticles can be altered by modulating the frequency response of surface electrons through changes in the shape of core-shell (*CS*) nanoinclusions (*NIs*).

Further research has investigated the plasmonic characteristics of spherical *CS* nanoparticles, including extinction, absorption, scattering cross-sections, and the field amplification factor [6,7]. This research considered variables such as distance from the center, angle, and

* Corresponding author e-mail: shewa.getachew@wku.edu.et

wavelength [8]. Additionally, studies have focused on how the dielectric properties of the surrounding medium and the depolarization factor affect optical bistability and absorption spectra in covered spherical *NCs* [9,10].

Significant nonlinear optical effects have been observed in plasmonic nanocomposites, including induced optical bistability (*OB*), where a single input field produces two distinct values of the local field intensity [11,12,13]. This effect is of great interest due to its potential applications in logic elements and optoelectronics [14]. Additionally, surface plasmon (*SP*) resonance, resulting from localized surface plasmonics, significantly strengthens the local electric field in these composites. The interaction between the localized surface plasmonics of the metallic shell and the dielectric core further amplifies the field enhancement. Laser light can generate these fields; however, when the incident electromagnetic wave frequency approaches the metal's *SP* frequency, the local field becomes abnormally amplified [16]. Although *OB* has made significant theoretical and experimental advances, further research is needed due to its many potential applications [17]. The local field enhancement at the focal point of spherical nanoinclusions in a linear dielectric host matrix was studied by [18]. Their study demonstrated that local field enhancement improves as the incident electromagnetic wave frequency approaches the metal inclusions *SP* frequency. By manipulating the metal thickness in coated inclusions, scientists can determine the maximum enhancement factor value. For dielectric-coated metal inclusions with a narrow dielectric shell and a thick metal core, the relevance of the enhancement factor increases [19].

Many studies have been conducted [20,21] to examine the effects of nanocomposites (*NCs*) on enhancement of the local field (*ELF*) and optical bistability, as well as their size, shape, composition, and spatial distributions [22,23]. Nevertheless, spheroidal core-shell *CS* geometries have not received as much attention as spherical or cylindrical *CS* nanoinclusions (*NIs*). The effects of the active and passive dielectric characteristics of the host matrices on local field enhancement and optical bistability have frequently been overlooked, even in studies involving *CS* nanocomposites [24,25,26]. Previous studies have demonstrated that the local field strengthening and optical bistability characteristics of *CS NCs* have been investigated using metal-coated dielectric materials as the core [27,28]. The influence of the dielectric properties of passive and active host matrices on the *ELF* and *OB* in cylindrical *NIs* has not been extensively explored. This study aims to investigate and evaluate the effects of metal fraction, as well as the dielectric properties of passive host matrices (*PHMs*) and active host matrices (*AHMs*), on *ELF* and *OB* in dielectric core-metallic shell, metallic core-dielectric shell, and pure metal cylindrical *NIs*.

2 Simulations and theoretical basis

We created a model, as shown in figure 1, using the quasistatic technique [29]. We next used theoretical and numerical analysis to investigate the *OB* and *ELF* properties of the model. Our research was centered on cylindrical *CS NIs*, in which the dielectric material with radius r_1 and dielectric function ε_h is used to form the core. In contrast, the shell has a radius of r_2, and ε_m, the applied electric field, determines its dielectric function (*DF*). The entire nanocomposite is exposed to incidental electromagnetic radiation while implanted in a dielectric host matrix with a *DF* of ε_h. We took into consideration two options for the host matrix's *DF* in order to investigate the impact on the increasing local field and optical bistability. A material's response to an applied electric field can determine whether the *DF*, represented by the symbol ε_h, is passive or active. The formula for this *DF* is [30]:

$$\varepsilon_h = \varepsilon_h' + i\varepsilon_h'' \tag{1}$$

ε_h' and ε_h'' represent the real and imaginary components of the *DF* of the host matrix material, respectively. The *DF* of the host matrix is regarded as passive when ε_h'' equals zero. Conversely, the dielectric function of the host matrix is deemed active when ε_h'' is smaller than zero. In order to evaluate each dielectric function's unique effects, we looked at both of its components independently in this study.

2.1 Distribution of electric potential in cylindrical core-shell NIs

The electric potential distribution in the core, shell, and host matrix was determined by solving the Laplace equations for cylindrical *CS NIs* and applying boundary condition criteria. Consider the *CS* nanocomposite materials depicted in Figure 1, where the dielectric core (*DC*) has a dielectric function (*DF*) ε_d and a radius r_1. The shell is defined by a dielectric function ε_m and radius r_2 (with $r_1 < r_2$). The host material is characterized by a dielectric function ε_h. The electric potential the distribution within the *DC*, metallic shell, and host matrix can be described by three separate functions: ϕ_d for the *DC*, ϕ_m for the metallic shell, and ϕ_h for the host matrix. These functions are derived according to the equation provided in reference [31].

$$\phi_d = -E_h A r\cos\theta, \qquad r \le r_1 \tag{2}$$

$$\phi_m = -E_h B r - \frac{C}{r}\cos\theta, \qquad r_1 \le r \le r_2, \tag{3}$$

$$\phi_h = -E_h\left(r - \frac{D}{r}\right)\cos\theta, \qquad r \ge r_2. \tag{4}$$

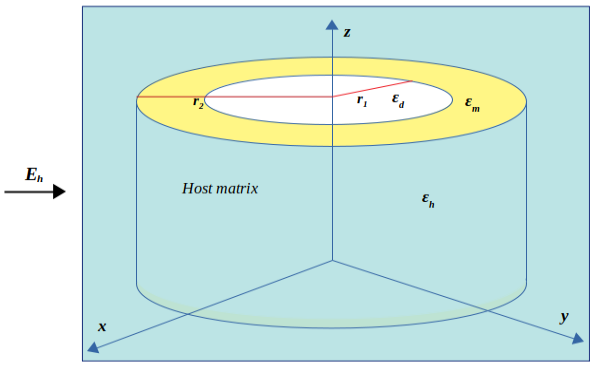

Fig. 1: The schematic figure shows a *CS* nanostructure consisting of a cylindrical dielectric particle with dielectric constant ε_d, covered by a metal shell with *DF* ε_m, embedded in a host matrix with *DF* ε_h.

Here, the applied electric field is denoted by E_h, and the cylindrical coordinates of the observation point are denoted by r and θ. The vector E_h is aligned with the z-axis. The values of the coefficients A, B, C, and D are not provided and must be determined using the continuity equations for the displacement vector and electric potential at the interfaces between the shell-host matrix and *CS* boundaries. The electric potential is continuous at the interface of a core-shell nanocomposite between the dielectric core (*DC*) and the metallic shell. This notion is based on the idea that the electric potential across the interface cannot change abruptly; therefore, the potential values in the dielectric (core) and metallic (shell) regions must be equal at the interface. This condition can be expressed as:

$$\phi_d = \phi_m, \quad r = r_1 \tag{5}$$

$$\phi_m = \phi_h, \quad r = r_2 \tag{6}$$

The continuity of the displacement vector (which is related to the electric field) must also be maintained at the interface. This condition can be expressed as:

$$\left.\frac{\partial \phi_m}{\partial r}\right|_{r=r_1} = \varepsilon_m \left.\frac{\partial \phi_d}{\partial r}\right|_{r=r_1} \tag{7}$$

$$\varepsilon_m \left.\frac{\partial \phi_m}{\partial r}\right|_{r=r_2} = \varepsilon_h \left.\frac{\partial \phi_h}{\partial r}\right|_{r=r_2} \tag{8}$$

where, the dielectric constants of the *DC*, metal shell, and dielectric host are denoted as ε_d, ε_m, and ε_h, respectively.

By solving equations (5), (6), (7), and (8) simultaneously, we can determine the values of the unknown coefficients listed below:

$$A = \frac{4\varepsilon_h \varepsilon_m}{p\nabla} \tag{9}$$

$$B = \frac{2\varepsilon_h(\varepsilon_d + \varepsilon_m)}{p\nabla} \tag{10}$$

$$C = \frac{2\varepsilon_h(\varepsilon_d - \varepsilon_m)}{p\nabla} r_1^2 \tag{11}$$

$$D = \left(1 - 2\varepsilon_h \frac{\varepsilon_m(2-p) + \varepsilon_d p}{p\nabla}\right) r_2^2 \tag{12}$$

Where, $p = 1 - \left(\frac{r_1}{r_2}\right)^2$ is the metal fraction in the inclusion,

$$\nabla = \varepsilon_m^2 + q\varepsilon_m + \varepsilon_d \varepsilon_h \tag{13}$$

$$q = \left(\frac{2}{p} - 1\right)(\varepsilon h + \varepsilon d) \tag{14}$$

The Drude-Sommerfeld model is a theoretical framework used to describe the behavior of electrons in a metal, providing a simplified yet effective way to understand the electrical and optical properties of metals. This model offers a straightforward expression for the dielectric function (DF) of the metal (ε_m). The dielectric function represents the material's response to an external electric field and determines its optical properties. From the Drude-Sommerfeld model, the *DF* of the metal (ε_m) is given by [25,35]:

$$\varepsilon_m = \varepsilon_\infty - \frac{1}{z(z+iz)} \tag{15}$$

Where, ε_∞ represents the impact of bound electrons on polarizability. Here, z is the ratio of incident radiation frequency (ω) to bulk plasma frequency (ω_p), and γ is the ratio of electron damping constant (ν) to plasma frequency (ω_p). Moreover, the real and imaginary parts of ε_m can be rewritten as

$$\varepsilon_m = \varepsilon_m' + i\varepsilon_m'' \tag{16}$$

Where,

$$\varepsilon_m' = \varepsilon_\infty' - \frac{1}{z^2+\gamma^2}, \quad \varepsilon_m'' = \varepsilon_\infty'' + \frac{\gamma^2}{z(z^2+\gamma^2)}$$

3 Enhancing local field of cylindrical *NIs*

In the quasi-static method, it is posited that the electric field E_h is uniform and aligned with the z-axis. Furthermore, it is stated that the local field within the core remains constant and can be calculated from the gradient of the electric potential inside the core [34,36].

$$E = -\nabla \Phi_d = AE_h \tag{17}$$

The mathematical expression of the enhancing local field (*ELF*) for different assemblages of the cylindrical *NIs* in terms of the dielectric constants and the metal volume fraction in the inclusion is presented in the following subsections.

3.1 Metal covered dielectric cylindrical NIs

The *ELF* in the *DC* is obtained by substituting equation (16) into equation (9), and then squaring and simplifying the resulting expression.

$$|A|^2 = \frac{16(\varepsilon_h'' - \varepsilon_h'')^2 + (\varepsilon_h'' + \varepsilon_h'')^2}{p^2[(\varepsilon_m' - \varepsilon_m' + q'\varepsilon_m - q''\varepsilon_m + \varepsilon_d\varepsilon_h)^2 + (2\varepsilon_d\varepsilon_m' + q'\varepsilon_m + q''\varepsilon_m + \varepsilon_d\varepsilon_h)^2]} \tag{18}$$

Where,

$$\varepsilon_h = \varepsilon_h' + i\varepsilon_h'', \quad q = q' + iq''$$
$$q' = \left(\frac{2}{p} - 1\right)(\varepsilon_d + \varepsilon_h), \quad q'' = -\left(\frac{2}{p} - 1\right)\varepsilon_h''$$

4 Dielectric covered metal cylindrical *NIs*

In the case of dielectric-coated metal cylindrical nanoinclusions (*NIs*), we can obtain the modified expression for the *ELF* by making a specific change to equation (9). This change involves replacing the dielectric constant ε_d with the dielectric constant of the metal ε_m, and replacing ε_m with ε_d in the equation. By doing so, we can derive the expression relevant to dielectric-coated metal cylindrical *NIs*, along with the corresponding schematic figure 2. Consider the core-shell (*CS*)

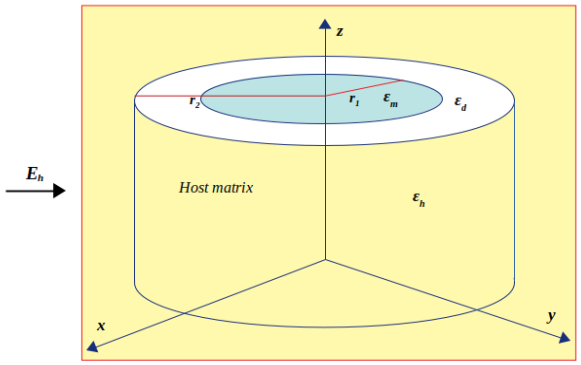

Fig. 2: The schematic figure shows a core-shell nanostructure consisting of a cylindrical dielectric particle with dielectric constant ε_d, coated by a metal shell with dielectric function ε_m, embedded in a host matrix with dielectric function ε_h.

nanoinclusions depicted in Figure 2, which consist of a dielectric core (*DC*) with a radius r_1 and dielectric permittivity ε_d, and a shell with a radius r_2 and dielectric permittivity ε_m. The host material has an electric permittivity ε_h. Consequently, the electric potential distributions within the metallic core (ϕ_m), dielectric shell (ϕ_d), and host matrix (ϕ_h) are expressed as follows:

$$\phi_m = -E_h A r\cos\theta, \qquad r \le r_1 \tag{19}$$
$$\phi_d = -E_h\left(Br - \frac{C}{r}\right)\cos\theta, \qquad r_1 \le r \le r_2 \tag{20}$$
$$\phi_h = -E_h\left(r - \frac{D}{r}\right)\cos\theta, \qquad r \ge r_2 \tag{21}$$

At the boundary between the dielectric shell and the metallic core of a *CS* nanoinclusions, the electric potential is continuous. This principle stems from the fact that there cannot be a sudden jump in electric potential across the interface; therefore, the potential values in the *CS* and shell-host matrix regions must be equal at the interface. This condition can be expressed as:

$$\phi_m = \phi_d, \qquad r = r_1 \tag{22}$$
$$\phi_d = \phi_h, \qquad r = r_2 \tag{23}$$

The continuity of the displacement vector which is related to the electric field is maintained at the interface. This condition can be expressed as:

$$\varepsilon_m\frac{\partial\phi_m}{\partial r} = \varepsilon_d\frac{\partial\phi_d}{\partial r}, \qquad r = r_1 \tag{24}$$
$$\varepsilon_d\frac{\partial\phi_d}{\partial r} = \varepsilon_h\frac{\partial\phi_h}{\partial r}, \qquad r = r_2 \tag{25}$$

Simultaneously solving equations (22), (23), (24), and (25) enables us to determine the values of the unspecified coefficients listed below:

$$A = \frac{4\varepsilon_h\varepsilon_d}{pV} \tag{26}$$
$$B = \frac{2\varepsilon_h(\varepsilon_m + \varepsilon_d)}{pV} \tag{27}$$
$$C = \frac{2\varepsilon_h(\varepsilon_m - \varepsilon_d)}{pV}r_1^2 \tag{28}$$
$$D = \left(1 - 2\varepsilon_h\frac{\varepsilon_d(2-p) + \varepsilon_m p}{pV}\right)r_2^2 \tag{29}$$

Where,

$$p = 1 - \left(\frac{r_1}{r_2}\right)^2 \tag{30}$$

$$\nabla = \varepsilon_d^2 + q\varepsilon_d + \varepsilon_m\varepsilon_h \tag{31}$$

$$q = \left(\frac{2}{p} - 1\right)(\varepsilon_h + \varepsilon_m) \tag{32}$$

Enhancing local field (*ELF*) for dielectric-coated cylindrical metal NIs is determined as follows:

$$|A|^2 = \frac{16(\varepsilon_h'^2 + \varepsilon_h''^2)\varepsilon_d^2}{p^2(\sigma'^2 + \sigma''^2)} \tag{33}$$

Where,

$$\varepsilon_h = \varepsilon_h' + i\varepsilon_h'',$$
$$\sigma' = \varepsilon_d^2 + q'\varepsilon_d + \varepsilon_m'\varepsilon_h' - \varepsilon_m''\varepsilon_h'', \quad \sigma'' = q''\varepsilon_d + \varepsilon_m'\varepsilon_h'' + \varepsilon_m''\varepsilon_h'$$
$$q' = \left(\frac{2}{p} - 1\right)(\varepsilon_d + \varepsilon_h'), \qquad q'' = \left(\frac{2}{p} - 1\right)\varepsilon_h''$$

4.1 Pure metal cylindrical NIs

For pure metal cylindrical *NIs*, we can formulate the equation associated with the depicted schematic figure 3. The potential distribution for pure metal cylindrical *NIs* with a radius of r_1 in a dielectric host matrix is given by:

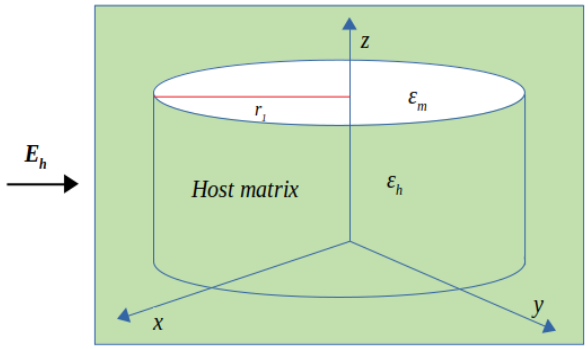

Fig. 3: The schematic figure shows a cylindrical pure metallic particle with dielectric function ε_m, coated by an embedded in a host matrix with dielectric function ε_h.

$$\Phi_m = -E_h A r cos\theta, \qquad r \le r_1 \tag{34}$$
$$\Phi_h = -E_h\left(r - \frac{B}{r}\right)\cos\theta, \qquad r \ge r_1 \tag{35}$$

Where, Φ_m represents the potential inside the cylinder, while Φ_h represents the potential outside the cylinder. The coefficients A and B are unknown and can be determined by applying the appropriate electrostatic boundary conditions.

$$A = \frac{2\varepsilon_h}{\varepsilon_h + \varepsilon_m} \tag{36}$$
$$B = \left(\frac{\varepsilon_m - \varepsilon_h}{\varepsilon_m + \varepsilon_h}\right) r_1^2 \tag{37}$$

So, the local field amplification factor for a cylindrical *NIs* made of pure metal is determined as:

$$|A|^2 = \frac{16(\varepsilon_h'^2 + \varepsilon_h''^2)}{(\varepsilon_m^2 + \varepsilon_h'^2) + (\varepsilon_h''^2 + \varepsilon_h'''^2)} \tag{38}$$

4.2 OB in metal covered dielectric Cylindrical NIs

When a dipole or polarization of charges forms on the surface of a nanoparticle due to the electric field created by the incident radiation, surface plasmons are created. One way to depict the local electric field E is as follows:

$$E = AE_h \tag{39}$$

Where, A - enhancement factor, E - local field, E_h - applied field

We investigate a metallic shell with a radius of r_2 surrounding a cylindrical dielectric particle, called the core, with a radius of r_1. With a nonlinear *DF*, the core is described as a Kerr type nonlinear dielectric material.

$$\varepsilon_d = \varepsilon_{d0} + \chi|E|^2 \tag{40}$$

The linear component of the *DF* is depicted by ε_{do}. The Kerr coefficient, represented by χ and found in Eq. (40), provides an explanation of the non-linear optical response of the core material. Understanding how the material behaves during nonlinear optical phenomena is largely dependent on this coefficient, which measures the strength of the dielectric profile's nonlinear response. Substituting Eq. (40) in to Eq. (13):

$$\nabla = \varepsilon_m + q\varepsilon_m + (\varepsilon_{d0} + \chi|E|^2)\varepsilon_h \tag{41}$$

Where

$$q = \left(\frac{2}{p} - 1\right)\varepsilon_{d0} + \left(\frac{2}{p} - 1\right)\chi|E|^2 + \left(\frac{2}{p} - 1\right)\varepsilon_h \tag{42}$$

Substitute Eq. (42) in to Eq. (41)

$$\nabla = \nabla_0 + \sigma\chi|E|^2 \tag{43}$$

where

$$V_0 = \varepsilon_m + \varepsilon_m q_0 + \varepsilon_{d0}\varepsilon_h \tag{44}$$
$$q_0 = \left(\frac{2}{p} - 1\right)\varepsilon_{d0} + \left(\frac{2}{p} - 1\right)\varepsilon_h \tag{45}$$
$$\sigma = \left(\frac{2}{p} - 1\right)\varepsilon_m + \varepsilon_h \tag{46}$$
$$V_0 = V_0' + iV_0'' \tag{47}$$
$$\varepsilon_h = \varepsilon_h' + i\varepsilon_h'' \tag{48}$$
$$\sigma = \sigma' + i\sigma'' \tag{49}$$
$$q_0 = q_0' + iq_0'' \tag{50}$$

By substituting the given value for the enhancing factor, we can derive the following result.

$$|A|^2 = \frac{16}{p^2}\left|\frac{\varepsilon_h\varepsilon_2^2}{\sigma}\right|^2\left[\frac{1}{|\nabla_0|^2 + 2\Re\left(\frac{\nabla_0}{\sigma}\right)\chi|E|^2 + |\chi|E|^2|^2}\right] \tag{51}$$

By squaring Eq. (30) multiply by χ we have

$$|\lambda E|^2 = |A|^2|\varepsilon_h|^2 \tag{52}$$

$$\chi|E|^2 = \frac{16}{p^2}\left|\frac{\varepsilon_h\varepsilon_m}{\sigma}\right|^2\left[\frac{\chi|E_h|^2}{|\frac{\nabla_0}{\sigma}|^2+2\Re\left(\frac{\nabla_0}{\sigma}\right)\chi|E|^2+|\chi|E|^2|^2}\right] \tag{53}$$

Let?s recall that the modulus of the *DF* of a *CS* nanocomposite is expressed as follows:

$$|\varepsilon_m'|^2 = |\varepsilon_m'|^2 + |\varepsilon_m''|^2$$
$$\varepsilon_m' = \varepsilon_\infty' - \frac{1}{z^2+\gamma^2}, \qquad \varepsilon_m'' = \varepsilon_\infty'' + \frac{\gamma}{z(z^2+\gamma^2)}$$
$$|V_0'|^2 = |V_0'|^2 + |V_0''|^2$$
$$V_0' = \varepsilon_m'' - \varepsilon_m' + q\varepsilon_m' + \varepsilon_d\varepsilon_h', \qquad V_0'' = 2\varepsilon_m'\varepsilon_m'' + q\varepsilon_m'' + \varepsilon_d\varepsilon_h''$$
$$|\sigma|^2 = |\sigma'|^2 + |\sigma''|^2$$
$$\sigma' = \left(\frac{2}{p}-1\right)\varepsilon_m' + \varepsilon_h', \qquad \sigma'' = \left(\frac{2}{p}-1\right)\varepsilon_m'' + \varepsilon_h''$$

And by obtaining $X = \chi|E|^2$ and $Y = \chi|E_h|^2$, the above equation becomes:

$$\eta Y = X^3 + aX^2 + bX \tag{54}$$

Where

$$\eta = \frac{16}{p^2}\left|\frac{\varepsilon_h\varepsilon_m}{\sigma}\right|^2, \qquad b = \left|\frac{\nabla_0}{\sigma}\right|^2, \qquad a = 2\Re\left(\frac{\nabla_0}{\sigma}\right)$$

5 Numerical Results and Discussion

The *DF* numerical values for the composite discussed in this section are sourced from references, with table 1 presenting the consistent values employed in numerical computations.

Table 1: Numerical values of physical quantities [21,22].

Numerical constant	*Values*
ε_d	6.0
ε_h	2.25
ε_∞	4.5
ω_p	1.6×10^{14}
ν	1.68×10^{16}
γ	1.15×10^{-3}

5.1 Impact of passive and active host matrix on ELF of metal covered dielectric cylindrical NIs

The *DF* of the host matrix affects the propagation and interaction of electromagnetic waves within the composite material. In a passive host matrix (*PHM*), the *DF* is typically constant and does not significantly modify the resonant behavior of the *NIs*. However, in an active host matrix (*AHM*), the *DF* can be tunable or exhibit anisotropic behavior, which can introduce additional degrees of freedom in shaping the resonant modes and thus impact the *ELF* peaks.

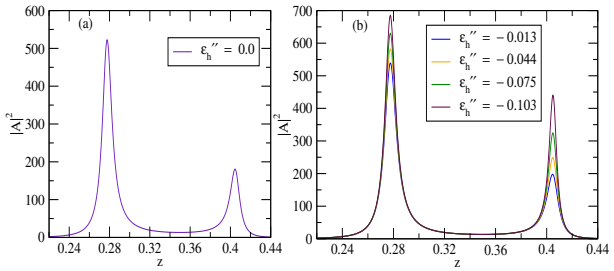

Fig. 4: Enhancin Local field ($|A|^2$) versus resonant frequency (z) of the cylindrical *NIs*: (a) in passive host matrix (*PHM*) and (b) in active host matrix (*AHM*) with p=0.9.

The investigation demonstrates that the *ELF* of cylindrical *NIs* exhibits two peaks in both the passive and *AHM* scenarios. This finding is illustrated in Figure 4(a) and (b), respectively. As the magnitude of the imaginary part of the *AHM* increases within the active embedded medium, from 0.013 to 0.103, the two peaks in the *ELF* of cylindrical *NIs* also shift to specific dimensionless frequencies (z). This behavior can be attributed to the fact

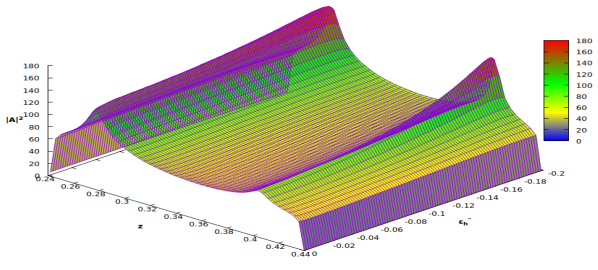

Fig. 5: The enhancement factor $|A|^2$ versus dimensionless frequency (z) and ε_h'' for a cylindrical *NIs* in *AHM*.

that the *AHM* retains the applied field as it propagates from the metallic shell to the *DC*. As a result, the number and intensities of the *ELF* peaks in cylindrical core-shell *NIs* exhibit significant variations depending on whether the host matrix is passive or active. By comparing Figures 4(a) and (b), it becomes evident that the passive and active *DFs* of the host matrix exert distinct effects on the *ELF* of cylindrical *NIs*. The investigation focused on

cylindrical *NIs* with an *AHM*, as depicted in Figure 4(b). The results demonstrate that as the value of ε_h'' increases, the *ELF* also increases. Specifically, when ε_h'' is set to 0.0, the LFEF value of the first peak is approximately 543 in the *PHM*. However, when the value of ε_h'' is increased to 0.103, the corresponding *ELF* rises to 692 in the *AHM*.

Overall, increasing the magnitude of the imaginary part of the surrounding medium in *AHMs* enhances the absorption, amplification, retention, and confinement of the electromagnetic field within the core-shell nanocavities. These factors collectively contribute to larger *ELF* values, indicating a stronger concentration and enhancement of the local electromagnetic field within the *AHM*. Although the physical quantities depicted in Figures 4 and 5 are identical, differences emerge between 2*D* and 3*D* graphs when considering idealized *AHMs*. This finding suggests that as the magnitude of the imaginary part of the host matrix increases, the *ELF* factor also rises, mirroring the trend observed in Figure 4.

5.2 The impact of metal fraction on ELF metal covered dielectric cylindrical NCs

We investigated the dependence of the *ELF* of core-shell *NIs* on the metal fraction. Regardless of whether passive or active host matrices were utilized, we saw changes in the *ELF* of cylindrical *NIs* as the metal concentration varied while holding the parameters constant. Figures

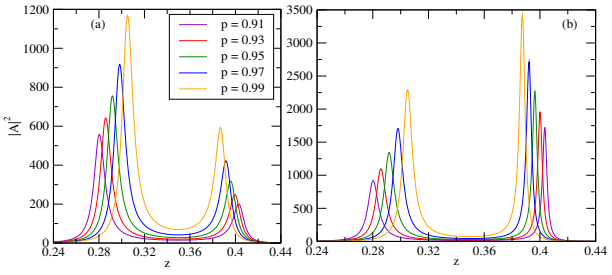

Fig. 6: The effect of the metal fraction on $(|A|^2)$ versus dimensionless resonant frequency (z) of the metal covered dielectric cylindrical *NIs*: (a) in *PHM* with ε_h'' =0.0 and (b) in *AHM* with ε_h'' = -0.1158911

6(a) and (b) illustrate these observations. Specifically, figure 6(a) demonstrates that the intensities of the peaks in the first set of *ELF* exhibit a blue shift and increase proportionally with the metal fraction in cylindrical *NIs* with a *PHM*. This suggests that these *ELF* peaks shift toward higher energy or shorter wavelengths at their peak positions. Similarly, we observed that the peaks in the second group experience a minor red shift in their intensities. This implies that these *ELF* peaks move toward longer wavelengths at their peak positions. The blue and red shifts of the *ELF* peaks indicate how the resonance properties of the *NIs* change in response to variations in metal content. These alterations can be attributed to modifications in the core-shell structure's localized electromagnetic field distribution, which in turn affects the interaction between the cylindrical *NIs* and incident light.

Thus, we investigated the relationship between the enhancing local field (*ELF*) of cylindrical nanoinclusions (*NIs*) and the dielectric function of the passive and active host materials (*AHM*). The findings showed that the effect of the host material's dielectric function on the *ELF* varies depending on whether the host matrix is passive or active. In particular, the intensity of the *ELF* increases in both the passive and active host matrix configurations with the same increase in the dielectric function of the host matrix (as illustrated in Figure 6).

It is clear from comparing Figures 6(a) and (b) that the *ELF* of cylindrical *NIs* is affected differently by the metal fraction as well as the passive and active dielectric functions of the host matrix. Specifically, increasing the metal content enhances the electromagnetic wave interaction capacity of cylindrical *NIs*. This increase also leads to a reduction in the power required for operation and in inter-particle distances, offering greater flexibility in material tuning. Accordingly, we conducted additional studies to understand the effect of varying the metal proportion on the *ELF* of cylindrical *NIs* in both passive and active host matrices. Our findings, shown in Figures 6(a) and (b), indicate that different *ELF* peak patterns are produced in the passive and active host matrices when the metal percentage is changed by the same amount. Further comparison of Figures 6(a) and (b) reveals that in active host matrices, the *ELF* value increases with the metal fraction (p). Additionally, the *ELF* of cylindrical *NIs* decreases as the core radius increases, i.e., when the metal fraction (p) decreases. These results are consistent with previous studies regarding the impact of metal fraction on *ELF* [25].

5.3 Dielectric coated metal cylindrical NIs

The figures presented below, specifically Figure 7, illustrate the relationship between the enhancement factor $(|A|^2)$ and the dimensionless frequency (z) for a composite material consisting of dielectric-coated metal cylindrical *NIs*. In this figure, the enhancement factor is observed to exhibit a single peak at a resonant frequency. The presence of this resonant frequency indicates the specific frequency at which the enhancement factor reaches its maximum value. This resonant behavior is closely related to the number of interfaces formed between the metallic portion of the *NIs* and the dielectric components of the composite material. The resonant frequency arises from the interaction between the incident electromagnetic waves and the composite structure. At this frequency, constructive interference occurs due to

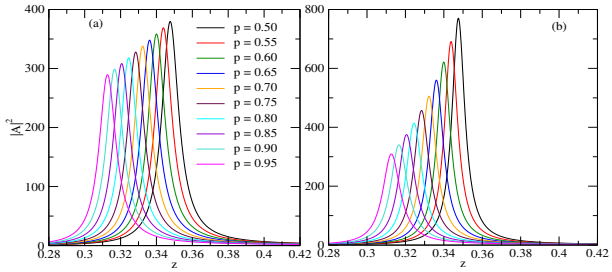

Fig. 7: The effect of the metal fraction on enhancing local field ($|A|^2$) versus dimensionless resonant frequency (z) of the dielectric coated metal cylindrical *NIs*: (a) in *PHM* with ε_h'' =0.0 and (b) in *AHM* with ε_h'' = -0.1158911

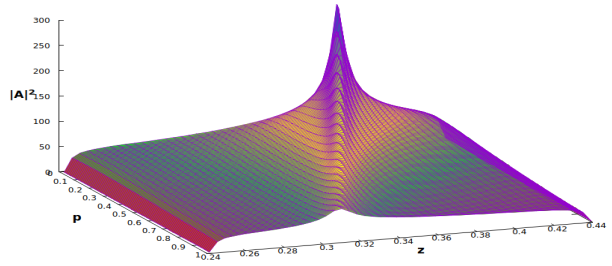

Fig. 8: The enhancement factor $|A|^2$ versus p and dimensionless frequency (z) for a cylindrical *NIs* in *AHM*.

appropriate phase matching between the incident waves and the scattered waves from the *NIs*. As a result, the enhancement factor reaches its highest value. Indeed, the dielectric shell of the *NIs* establishes interfaces with both the host dielectric and the metallic core. Consequently, the free electrons within the metallic core oscillate at the surface plasmon frequency, which is consistent along the interface of the shell dielectric.

As shown in Figure 7, there is only one dimensionless resonant frequency and one maximum value of the enhancement factor in a composite material composed of metal cylinders coated with dielectric *NIs*. To achieve a greater enhancement factor in this type of composite, varying the thickness of the metal component is essential. While the physical quantities depicted in Figures 7 and 8 are the same, discrepancies between the 2D and 3D graphs become apparent when idealized *AHMs* are considered. This result implies that the *ELF* factor decreases with increasing metal content, consistent with the pattern shown in Figure 7. In particular, Figure 7(a) illustrates the situation of a *PHM* with no imaginary permittivity component ($\varepsilon_h'' = 0$). It shows that the enhancement factor increases dramatically in magnitude when the metallic percentage decreases from 0.95 to 0.50. Consequently, the incident field is amplified beyond the range of 281 to 376 due to this rise in the enhancement factor. In an active host matrix, where the imaginary

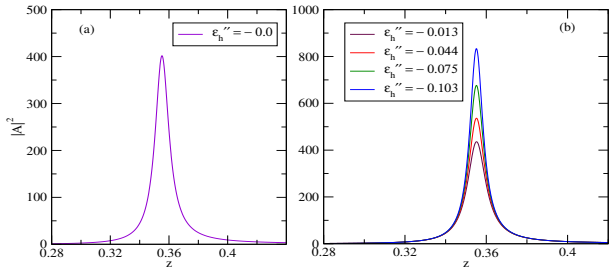

Fig. 9: The effect of the ε_h'' on $|A|^2$ versus dimensionless resonant frequency (z) of the dielectric coated metallic cylindrical *NIs*: (a) in *PHM* with ε_h'' =0.0 and (b) in *AHM* with four different ε_h''.

component of permittivity (ε_h'') is non-zero, Figure 7(b) highlights the *ELF*. In this case, the enhancement factor also shows a notable increase in magnitude as the metallic fraction decreases from 0.95 to 0.50. As a result, the enhancement of the incident field extends beyond the range of 304 to 783. The numerical calculations indicate that, for the same dielectric parameter and metal fraction value, the magnitude of the enhancement factor in an *AHM* increases to 783 within the region of the dimensionless resonant frequency ($z = 0.35$).

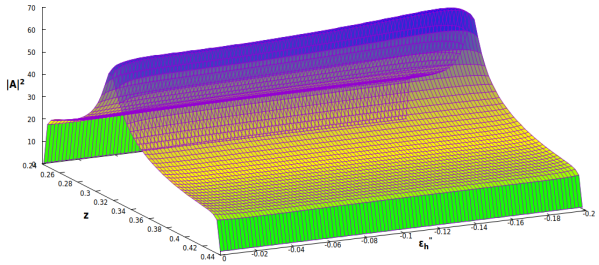

Fig. 10: The effect of the ε_h'' on $|A|^2$ versus dimensionless resonant frequency (z) of the dielectric covered metal cylindrical *NIs* in *AHM*.

By affecting the resonant frequency, Figures 9 (a) and (b) demonstrate the important roles that the dimensionless metal proportions (p) and the imaginary component of the dielectric function of an *AHM* play in determining local field amplification. This result implies that a composite material with metallic cylindrical *NIs* coated in metal exhibits a single maximal enhancement factor value and a single resonant frequency. The interaction between electromagnetic waves and the structure can be modified by adjusting the dielectric characteristics of the host matrix material. A larger local field enhancement factor results from effectively enhancing the confinement of electromagnetic fields within the structure through an increase in optical density. The $|A|^2$ is approximately 405

in the case of a passive host matrix ($\varepsilon_h'' = 0$), as shown in Figure 9(a). Numerical simulations show a considerable increase in the size of $|A|^2$ from 420 to 851 in an *AHM* when the magnitude of the imaginary part of the *AHM* (ε_h'') increases from 0.013 to 0.103. Figures 9 and 10 display identical physical quantities, but differences between the 2*D* and 3*D* graphs become evident when idealized *AHMs* are considered. According to this finding, the *ELF* factor increases as the magnitude of ε_h'' rises, which is consistent with the pattern seen in Figure 9.

5.4 Pure metal cylindrical NIs

The dielectric function of the passive or active host matrix is the main factor that determines the enhancement factor for pure metal *NIs*. When a host matrix is passive and lacks an imaginary component of permittivity ($\varepsilon_h'' = 0$), the real part of the dielectric function predominantly affects the enhancement factor. The way electromagnetic waves interact with the metal *NIs* and influence the confinement and amplification of the local field is determined by the dielectric characteristics of the passive host matrix. In an *AHM* where the imaginary part of the dielectric function is non-zero, both the real and imaginary components contribute to the enhancement factor. The real component affects the amplification of the local field and the resonance frequency, while the imaginary component influences the absorption and dissipation of energy within the composite structure.

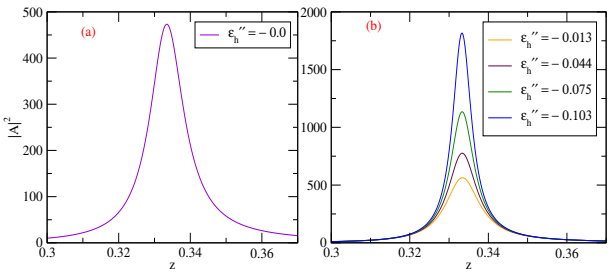

Fig. 11: The effect of the ε_h'' on $|A|^2$ versus dimensionless resonant frequency (z) of the pure metal cylindrical *NIs*: (a) in *PHM* with ε_h'' =0.0 and (b) in *AHM* with four different ε_h''.

Figures 11 (a) and (b) show that the enhancement factor at a given resonant frequency has a single maximum value. The local field enhancement ($|A|^2$) reaches approximately 475 in the case of a *PHM*, as shown in figure 11 (a). This value represents the highest possible improvement if the dielectric function of the host matrix does not include an imaginary component. Furthermore, there is a noticeable increase in the enhancement factor's magnitude with an increase in the imaginary component of the *AHM*.

In contrast, for an *AHM*, numerical computations show a significant increase in the size of $|A|^2$, from 500 to 1842, as the magnitude of the imaginary part of the active host matrix (ε_h'') rises from 0.013 to 0.103, as shown in figure 11 (b). This increase in the enhancement factor suggests that the local field can be significantly enhanced by an active host matrix with a non-zero imaginary part of the dielectric function.

5.5 OB in metal covered dielectric cylindrical NIs

Whether passive or active, the *DF* of the host matrix is an important factor affecting optical bistability (*OB*) in *NIs*. In this section, we examine the effects of varying the imaginary part of the *AHM* in cylindrical *NIs*. We conducted investigations with different values of ε_h'', while maintaining a constant dimensionless metal fraction (p). As shown in Figure 12, the outcomes for cylindrical core-shell *NIs* with both passive and *AHMs* were compared. The results indicate that, for an *AHM*, the switching-up threshold field increases proportionally with the magnitude of the imaginary component of the *AHM* (ε_h''). In contrast, this effect is absent in the *PHM* where $\varepsilon_h'' = 0.0$.

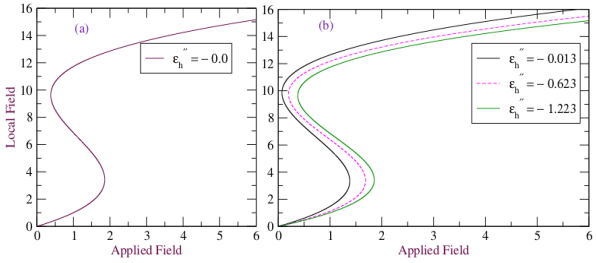

Fig. 12: The effect of the ε_h'' on optical bistability of metal coated dielectric cylindrical *NIs*: (a) in *PHM* with ε_h''=0.0 and (b) in *AHM* with different ε_h''.

As an illustration, the appropriate applied field value is roughly 1.4 when the magnitude of ε_h'' is 0.013. On the other hand, the corresponding switching-up threshold fields in *AHMs* increase to 1.86 when the magnitude of ε_h'' is increased to 1.233. Thus, the switching-up threshold of *IOB* of cylindrical *NIs* also happens at large values of incident field for large values of imaginary part of *AHM* (ε_h''). However, it can be seen that, particularly in active host matrices, increasing the dielectric characteristics of the surrounding medium results in a broader switching-down threshold field.

The features of their optical bistability reveal some intriguing patterns when we change the metal fraction in

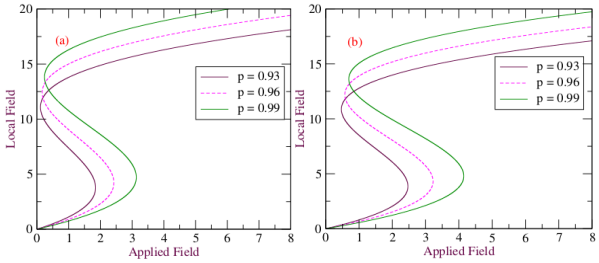

Fig. 13: The effect of the metal fraction on optical bistability of metal coated dielectric cylindrical *NIs*: (a) in *PHM* with ε_h'' =0.0 and (b) in *AHM* with ε_h'' = -1.233.

NIs. Specifically, they become more responsive in adjusting material properties, require lower operating power, and show an improved capacity to interact with electromagnetic waves as the metal percentage increases. Therefore, we examined the impact of varying the metal proportion on the optical bistability (OB) of cylindrical core-shell *NIs* using both passive and active host matrices. Figures 13(a) and (b) demonstrate that different peaks and bistability zones of OB are generated in passive and active host matrices by fixing the values of ε_h'' and varying the metal fraction by the same amount. Both passive and active host matrices require a higher incident field at any switching-up criteria point as the metal fraction increases.

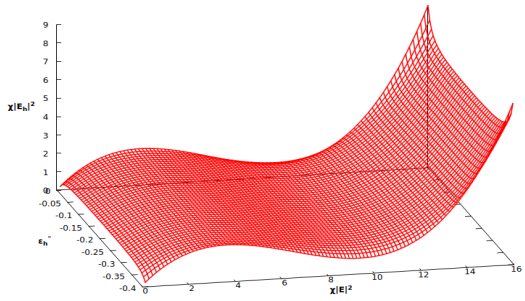

Fig. 14: Local field ($\chi|E|^2$) versus applied field ($\chi|E|^2$) at resonate frequency (z) = 0.2, with parameters, ε_h''= 2.25, γ = 0.0115 for a cylindrical nanoinclusions in *AHM*.

On the other hand, the switching-down points occur at almost the same incident electromagnetic field for different values of the metal fraction (p). A closer examination of the results from Figure 13 reveals that active host matrices have higher applied field values at which the switching-up of *OB* occurs for each value of the metal fraction. The bistable threshold of cylindrical *NIs* decreases with an increasing core radius, that is, with a decreasing p, which results in smaller bistable outputs (Figure 13). Conversely, as the metal fraction increases, so does the switching-up threshold field, resulting in a broader bistable area. Therefore, by modifying the metal fraction or size of the *NIs*, it is possible to regulate the *OB* in passive and *AHMs*. Regarding the effect of the metal fraction on *OB*, the study's findings are consistent with previous investigations [25,34]. Although the physical quantities depicted in Figures 12 and 14 are identical, considering idealized *AHMs* reveals discrepancies between the 2*D* and 3*D* graphs.

6 Conclusions

In this study, we investigated the optical properties of cylindrical nanoinclusions embedded in both passive and active host matrices. We then conducted a theoretical and numerical analysis of the enhancement of the local field and optical bistability of the system using the quasistatic approximation. When considering composites with metal-covered dielectric *NIs*, two distinct resonant frequencies exhibit two peak values of the enhancement factor. In contrast, for composites with dielectric-covered metal and pure inclusions, there is only a single maximum value of the enhancement factor. For metal-covered dielectric *NIs* with a thick metal cover and an increasing imaginary part of the host matrix (represented as ε_h''), the enhancement factor becomes more significant. Similarly, for dielectric-coated metal *NIs* with a thin metal core and an increasing imaginary part of the host matrix, the enhancement factor also becomes more pronounced. In contrast, the magnitude of the enhancement factor in pure metal *NIs* is solely determined by the imaginary part of the dielectric properties of the host matrix. As the imaginary part of the host matrix increases, there is a substantial increase in the amplification of the enhancement factor. We also conducted an investigation by varying the values of p and the imaginary part of the host matrix (ε_h''), and utilized the root analysis approach to explore changes in induced optical bistability within cylindrical metals covered with dielectric *NIs* with passive and *AHMs*. The results indicate that induced *OB* in cylindrical *NIs* is achieved at a lower applied field in *PHMs* compared to active ones, regardless of changes in p or ε_h''. However, the *OB* region is relatively narrower in *PHMs* and broader in *AHMs* with dielectric properties. As the metal fraction increases, the incident field required at each switching-up threshold point also increases in both passive and *AHMs*, resulting in a wider bistable region. These findings suggest that optical bistability in both passive and *AHMs* can be controlled by adjusting the metal fraction of the cylindrical *NIs*. Additionally, the study suggests that as the value of ε_h'' increases, the switching-up threshold for the *OB* of cylindrical *NIs* occurs at higher values of the incident field. These findings present exciting prospects for the utilization of these nanoinclusions in practical applications, including optical sensing, nonlinear optics, quantum optics, optical circuits, logic operations, and optical memories.

Data Availability

This manuscript has no associated data or the data will not be deposited.

Conflicts of Interest

The authors have no conflicts to declare.

Author Contributions

Shewa Getachew: Conceptualization (equal contribution); Data curation (equal contribution); Formal analysis (equal contribution); Investigation (equal contribution); Methodology (equal contribution); Software (equal contribution); Writing - original draft (equal contribution); Writing - review & editing (equal contribution). **Hawi Aboma:** Conceptualization (equal contribution); Formal analysis (equal contribution); Methodology (equal contribution); Investigation (equal contribution).

Funding Statement

No funding was received for conducting this study.

Ethics conduct

Not applicable.

ORCID iD

Shewa Getachew: orcid.org/0009-0005-8265-0115

References

[1] Stalmashonak, A., Seifert, G., & Abdolvand, A. (2013). Ultra-short pulsed laser engineered metal-glass nanocomposites (pp. 5-15). New York, NY, USA: Springer.

[2] Amendola, V., Pilot, R., Frasconi, M., Maragò, O. M., & Iatì, M. A. (2017). Surface plasmon resonance in gold nanoparticles: a review. *Journal of physics: Condensed matter*, 29(20), 203002.doi: 10.1088/1361-648X/aa60f3

[3] Getachew, S. (2024). Effect of Tunable Dielectric Core on Optical Bistability in Cylindrical Core?Shell Nanocomposites. *Advances in Condensed Matter Physics*, **2024**(1), 9911970.doi: https://doi.org/10.1155/2024/9911970

[4] Volz, T., Reinhard, A., Winger, M., Badolato, A., Hennessy, K. J., Hu, E. L., & Imamo?lu, A. (2012). Ultrafast all-optical switching by single photons. *Nature Photonics*, 6(9), 605-609.

[5] Zhang, Y. X., & Wang, Y. H. (2017). Nonlinear optical properties of metal nanoparticles: a review. *RSC advances*, 7(71), 45129-45144.

[6] Ali, B. M. (2024). Tunable optical properties of graphene wrap**11**(7), 075001.doi: 10.1088/2053-1591/ad5cda

[7] Jafarzadeh, H., Sahrai, M., & Jamshidi-Ghaleh, K. (2014). Controlling the optical bistability in a ?-type atomic system via incoherent pump field. *Applied Physics B*, 117, 927-933.

[8] Hértilli, S., Yahyaoui, N., Zeiri, N., Baser, P., Said, M., & Saadaoui, S.(2024). Theoretical modeling of nonlinear optical properties in spheroidal CdTe/ZnTe core/shell quantum dot embedded in various dielectric matrices. *Results in Physics*, **56**, 107274.

[9] Piralaee, M., Asgari, A., & Siahpoush, V. (2018). Plasmonic properties of spheroid silicon-silver nanoshells in prolate and oblate forms. *Optik*, 172, 1064-1068.doi: https://doi.org/10.1016/j.ijleo.2018.07.131

[10] Getachew, S., & Berga, G. (2024). Investigating the optical bistability of pure spheroidal nanoinclusions in passive and active host matrices. *Canadian Journal of Physics*.doi: https://doi.org/10.1139/cjp-2024-0144

[11] Haus, J. W., Kalyaniwalla, N., Inguva, R., & Bowden, C. M. (1989). Optical bistability in small metallic particle composites. *Journal of applied physics*, 65(4), 1420-1423.doi: https://doi.org/10.1063/1.342979

[12] Arnold, S., O?Keeffe, T. R., Leung, K. M., Folan, L. M., Scalese, T., & Pluchino, A. (1990). Optical bistability of an aqueous aerosol particle detected through light scattering: theory and experiment. *Applied optics*, 29(24), 3473-3478.doi: https://doi.org/10.1364/AO.29.003473

[13] Neuendorf, R., Quinten, M., & Kreibig, U. (1996). Optical bistability of small heterogeneous clusters. *The Journal of chemical physics*, 104(16), 6348-6354.doi: https://doi.org/10.1063/1.471296

[14] Movsisyan, A., & Parsamyan, H. (2024). Gap-enhanced optical bistability in plasmonic core-nonlinear shell dimers. Nanoscale, 16(4), 2030-2038.doi: DOI https://doi.org/10.1039/D3NR04237E

[15] Getachew, S. (2024). Investigation of refractive index and group velocity of metal coated dielectric spherical nanocomposites within both passive and active dielectric cores. *Iranian Journal of Physics Research*, **24**(3), 75-87.doi: https://doi.org/10.47176/ijpr.24.3.51890

[16] Buryi, O. A., Grechko, L. G., Mal?nev, V. N., & Shewamare, S. (2011). Induced optical bistability in small metal and metal coated particles with nonlinear dielectric functions. *Ukrainian Journal of Physics*, 56(4), 311-311.doi: https://doi.org/10.15407/ujpe56.4.311

[17] Szöke, A., Daneu, V., Goldhar, J., & Kurnit, N. A. (1969). Bistable optical element and its applications. *Applied Physics Letters*, 15(11), 376-379.doi: https://doi.org/10.1063/1.1652866

[18] Miller, D., Smith, S., & Seaton, C. (1981). Optical bistability in semiconductors. *IEEE journal of quantum electronics*, **17**(3), 312-317.

[19] Mal'nev, V. N., & Shewamare, S. (2013). Slow and fast light in metal/dielectric composites with passive and active host matrices. *Physica B: Condensed Matter*, 426, 52-57.doi: https://doi.org/10.1016/j.physb.2013.06.013

[20] Fischer, G. L., Boyd, R. W., Gehr, R. J., Jenekhe, S. A., Osaheni, J. A., Sipe, J. E., & Weller-Brophy,

L. A. (1995). Enhanced nonlinear optical response of composite materials. *Physical review letters*, 74(10), 1871.doi: https://doi.org/10.1103/PhysRevLett.74.1871

[21] Zhu, J., & Zhao, S. M. (2016). Plasmonic refractive index sensitivity of ellipsoidal Al nanoshell: Tuning the wavelength position and width of spectral dip. *Sensors and Actuators B: Chemical*, 232, 469-476.doi: https://doi.org/10.1016/j.snb.2016.03.163

[22] Chen, H. L., Gao, D. L., & Gao, L. (2016). Effective nonlinear optical properties and optical bistability in composite media containing spherical particles with different sizes. *Optics Express*, 24, 5334-5345.doi: 10.1364/OE.24.005334

[23] Shewamare, S., & Mal'nev, V. N. (2012). Two optical bistability domains in composites of metal nanoparticles with nonlinear dielectric core. *Physica B: Condensed Matter*, **407**, 4837-4842.doi: https://doi.org/10.1016/j.physb.2012.08.007

[24] Bergaga, G. D., Ali, B. M., & Debela, T. S.(2023). Effects of shape on the optical properties of CdSe@ Au core-shell nanocomposites. *AIP Advances*, **13**.doi: https://doi.org/10.1063/5.0138456

[25] Getachew, S., Shewamare, S., Diriba, T., & Berhanu, G. (2023). Local field enhancement of cylindrical core-shell nanoparticle composites in active and passive dielectric core. *International Journal of Current Research*, **15**, 26432-26438.doi: DOI: https://doi.org/10.24941/ijcr.45824.11.2023

[26] Kalyaniwalla, N., Haus, J. W., Inguva, R., & Birnboim, M. H. (1990). Intrinsic optical bistability for coated spheroidal particles. *Physical Review A*, **24**, 5613.doi: https://doi.org/10.1103/PhysRevA.42.5613

[27] Hirpha, T. T., Bergaga, G. D., Ali, B. M., & Gebre, S. S. (2024). Investigation of optical bistability in spheroidal core-shell nanocomposites with passive and active dielectric cores. *AIP Advances*, **14**(1).doi: https://doi.org/10.1063/5.0180907

[28] Nugroho, B. S., Iskandar, A. A., Malyshev, V. A., & Knoester, J. (2020). Plasmon-assisted two-photon absorption in a semiconductor quantum dot-metallic nanoshell composite. *Physical Review B*, **102**, 045405.doi: https://doi.org/10.1103/PhysRevB.102.045405

[29] Gao, L.(2003). Optical bistability in composite media with nonlinear coated inclusions. *Physics Letters A*, **318**, 119-125.doi: https://doi.org/10.1016/j.physleta.2003.09.025

[30] Larsson, J.(2007). Electromagnetics from a quasistatic perspective. *American Journal of Physics*, **75**, 230-239.doi: https://doi.org/10.1119/1.2397095

[31] Rothwell, E. J., Frasch, J. L., Ellison, S. M., Chahal, P., & Ouedraogo, R. O.(2016). Analysis of the Nicolson-Ross-Weir method for characterizing the electromagnetic properties of engineered materials. *Progress In Electromagnetics Research*, **157**, 31-47.doi: doi:10.2528/PIER16071706

[32] Buryi, O. A., Grechko, L. G., Malnev, V. N., & Shewamare, S. (2011). Induced Optical Bistability in Small Metal and Metal Coated Particles with Nonlinear Dielectric Functions. *Ukrainian Journal of Physics*, **56**, 311-311.doi: https://doi.org/10.15407/ujpe56.4.311

[33] Jule, L., Mal'nev, V., Mesfin, B., Senbeta, T., Dejene, F., & Rorro, K. (2015). Fanolike resonance and scattering in dielectric (core)-metal (shell) composites embedded in active host matrices. *physica status solidi (b)*, **252**, 2707-2713.doi: https://doi.org/10.1002/pssb.201552221

[34] Pan, T., & Li, Z. Y. (1999). Optical bistability of metallic particle composites. *physica status solidi (b)*, **213**, 203-210.doi: https://doi.org/10.1002/(SICI)1521-3951(199905)213:1¡203::AID-PSSB203¿3.0.CO;2-H

[35] Aboma, H. (2025). Effect of Tunable Dielectric Function of the Core on Optical Bistability in Small Spherical Metal-Dielectric Composite. Jefore Ethiopian Journal of Applied Sciences.doi: https://doi.org/10.70984/dgr2qq38

[36] Atnaf, T. & Getachew, S. (2024). Investigation Optical Properties of ZnTe@Ag Core-Shell Spherical Nanocomposites Within Varies Dielectric Host Matrices. *Adv Mater.*, 13(4):80-91. doi: doi: 10.11648/j.am.20241304.13